

# Do Thermoelectric Materials in Nanojunctions Display Material Property or Junction Property?

Yu-Chang Chen and Yu-Shen Liu

Department of Electrophysics, National Chiao Tung University, 1001 Ta Hsueh Road, Hsinchu 30010, Taiwan

The miniaturization of thermoelectric nanojunctions raises a fundamental question: do the thermoelectric quantities of the bridging materials in nanojunctions remain to display material properties or show junction properties? In order to answer this question, we investigate the Seebeck coefficient  $S$  and the thermoelectric figure of merit  $ZT$  especially in relation to the length characteristics of the junctions from the first-principles approaches. For  $S$ , the metallic atomic chains reveal strong length characteristics related to strong hybridization in the electronic structures between the atoms and electrodes, while the insulating molecular wires display strong material properties due to the cancelation of exponential scalings in the DOSs. For  $ZT$ , the atomic wires remain to show strong junction properties. However, the length characteristics of the insulating molecular wires depend on a characteristic temperature  $T_0 = \sqrt{\hbar^2 / (k_B m^*)}$  around 10 K. When  $T \ll T_0$ , where the electron transport dominates the thermal current, the molecular junctions remain to show material properties. When  $T \gg T_0$ , where the phonon transport dominates the thermal current, the molecular junctions display junction properties.

Nanoscale thermoelectric devices can be considered as the new types of devices which can be embedded into integrated chip sets to assist the stability of devices by converting the accumulated waste heat into useful electric energy. There has been an ever increasing interest in the thermoelectric properties of nanojunctions [1, 2, 3, 4, 5, 6, 7, 8, 9, 10], partially motivated by the recent experiments demonstrating the capability of measuring the Seebeck coefficients in the molecular junctions [11, 12]. As the Seebeck coefficients are relevant not only to the magnitude but also to the slope of density of states (DOSs), they can reveal more detailed information about the electronic structures of the materials sandwiched in the nanojunctions beyond what the conductance measurements can provide. The Seebeck coefficients have been applied to explore the electronic structures of molecular junctions using functional substitutions for the bridging molecules [10, 12]. Theorists have proposed using gate fields and external biases as means to modulate the Seebeck coefficients in nanojunctions [2, 3, 10]. Much research has been devoted to the study of Seebeck coefficients [1, 2, 3, 4, 5, 6, 7, 8, 9, 10], but little is known about the fundamental thermoelectric properties in nanojunctions.

Indeed, the miniaturization of thermoelectric nanojunctions raises a fundamental question: does bridging thermoelectric material in nanojunctions show material properties or junction properties? Thermoelectric bulk crystals usually show material properties, where the thermoelectric physical quantities are irrelevant to the sizes and shapes of materials. In addition, recent experiments on Seebeck coefficients in molecular junctions also reveal strong signals of material properties. These experiments have observed that Seebeck coefficients are insensitive to the number of molecules in junctions and show rather weak dependence on the lengths of the bridging molecules, which is in sharp contrast to the conductance which shows strong exponential dependence on the lengths of molecules [11, 12, 13]. However, the bridg-

ing materials in nanojunctions may have strong interactions with the contacts. From this point of view one can say thermoelectric quantities can display the junction characteristics. Considering the examples and the reason quoted above, it is therefore not obvious whether the thermoelectric quantities of the bridging materials in nanojunctions display junction properties or material properties.

In this letter, we will show that the thermoelectric quantities in nanojunctions unnecessarily display entire material properties or junction properties. To demonstrate this point, this study investigates two important thermoelectric quantities, the Seebeck coefficient ( $S$ ) and the thermoelectric figure of merit ( $ZT$ ), in (metallic) aluminum atomic junctions and (insulating) molecular junctions. It shows that metallic atomic chains reveal strong junction properties while the insulating molecular wires partially possess the material properties, where  $S$  reveals the material property and  $ZT$  displays the junction property at temperatures larger than the characteristic temperature  $T_0$ .

To answer the question, we have developed a theory with analytical expressions for  $S$  and  $ZT$  allied to a fully self-consistent first-principles calculation in the framework of the density functional theory (DFT). It allows us to numerically calculate  $S$  and  $ZT$  and subsequently investigate these quantities analytically. We focus on the subject on whether  $S$  and  $ZT$  depend on the characteristics of the junctions, especially on the dependence on length-characteristic of junctions. Before turning to the detailed discussion, let us begin with a brief introduction on how to calculate  $S$  and  $ZT$ . First, we consider that the junction consists of source-drain electrodes, with distinct chemical potentials  $\mu_{L(R)}$  and temperatures  $T_{L(R)}$ , as independent electron and phonon reservoirs. When an additional infinitesimal temperature  $T$  is applied across the junction, an extra voltage  $V$  is induced to compensate the electric current induced by the temperature gradient  $\nabla T$  across the junction. We then derive the

expressions for  $S$  (defined as  $S = \frac{V}{I} = T$ ) and the electron thermal conductance (defined as  $\kappa_{el} = \frac{J_Q^{e1}}{T}$ ), where  $J_Q^{e1}$  is the thermal current conveyed by the electrons which also carry the electric current).

$$S = \frac{1}{e} \frac{\frac{K_L^L}{T_L} + \frac{K_R^R}{T_R}}{K_0^L + K_0^R}; \quad (1)$$

$$\kappa_{el} = \frac{1}{h} \sum_{i=L,R} X_i (K_1^i eS + \frac{K_2^i}{T_i}); \quad (2)$$

where  $K_n^{L(R)} = \int dE E^n \Gamma_{L(R)} \frac{\partial f_E^{L(R)}}{\partial E}$ , and the transmission function  $\Gamma(E) = \Gamma^R(E) = \Gamma^L(E)$ , which is a direct consequence of the time-reversal symmetry. It has been assumed that the left and right electrodes serve as independent electron and phonon reservoirs where the electron population is described by the Fermi-Dirac distribution function,  $f_E^{L(R)} = 1 / \exp(E - \mu_{L(R)} / k_B T_{L(R)} + 1)$ , and  $k_B$  is the Boltzmann constant. The transmission functions are computed using the wave functions obtained self-consistently in the DFT framework [14, 15]. We should notice that the above equations are suitable for describing  $S$  and  $\kappa_{el}$  in nanojunctions operated under finite external biases, where two electrodes can have different temperatures.

In addition, the differential conductivity, typically insensitive to temperature in cases where direct tunneling is the major transport mechanism, can be expressed as

$$\frac{dI}{dV} = \frac{e}{2} \sum_{i=L,R} \int dE X_i f_E^i (1 - f_E^i) \Gamma(E) / k_B T_i; \quad (3)$$

So far, the physical quantities ( $S$ ,  $\kappa_{el}$ , and  $\kappa_{ph}$ ) which have been discussed are related to the electron transport. It must be noted that the heat current is conveyed by the electrons and phonons simultaneously. The phonon thermal conductance ( $\kappa_{ph}$ ) usually dominates the combined thermal conductance  $\kappa = \kappa_{el} + \kappa_{ph}$  at large temperatures. The complete discussion on  $ZT$  shall include the essential ingredient  $\kappa_{ph}$ ; thus  $ZT$  can be expressed as follows:

$$ZT = \frac{S^2}{\kappa_{el} + \kappa_{ph}} T; \quad (4)$$

where  $T = (T_L + T_R)/2$  is the average temperature of the source-drain electrodes. We estimate the phonon thermal conductance following the approaches of Pattachan and Geller [16]. It is assumed that the nanojunction is a weak elastic link, with a given stiffness which can be evaluated from the total energy calculations, attached to the electrodes modeled as phonon reservoirs. The phonon thermal conductance (defined by  $\kappa_{ph} = \frac{J_Q^{ph}}{T}$ ) is given by:

$$\kappa_{ph} = \frac{K^2}{k_B} \sum_{i=L,R} \int dE E^2 N_L(E) N_R(E) X_i \frac{n_i(E) (1 + n_i(E))}{T_i^2}; \quad (5)$$

where  $n_L(R) = 1 / \exp(E - \mu_{L(R)} / k_B T_{L(R)} + 1)$  and  $N_{L(R)}(E)$  is the Bose-Einstein distribution function and the spectral density of phonon states in the left (right) electrode, respectively. The stiffness of the bridging nanostructure is  $K = YA/l$ , where  $Y$  is the Young's modulus and  $A(l)$  is its cross-section (length).

We have numerically computed  $S$  and  $ZT$  using Eqs. (1) to (5) allied to the transmission functions obtained self-consistently in the DFT framework, as shown in Figs. 1 and 2. To elaborate the properties of the Seebeck coefficient and the thermoelectric figure of merit, we will limit our discussion to the linear response regime (i.e.,  $\mu_L = \mu_R = \mu$ ) and  $T_L = T_R = T$ . After expanding  $S$ ,  $\kappa_{el}$ , and  $\kappa_{ph}$  in terms of the temperature  $T$ , we obtain the analytical expressions for the  $S$  and  $ZT$ .

$$S = \frac{1}{e} \frac{2k_B^2}{T} \frac{\partial \Gamma(E)}{\partial E} \Big|_{E=\mu}; \quad (6)$$

where  $\frac{\partial \Gamma(E)}{\partial E} \Big|_{E=\mu} = \frac{\partial \Gamma(E)}{\partial E} \Big|_{E=\mu} = \frac{\partial \Gamma(E)}{\partial E} \Big|_{E=\mu}$ . We have noted that the Seebeck coefficient depends on the magnitude and the slope of the transmission function, and is linearly proportional to  $T$  at low temperatures.

$$ZT = \frac{S^2 T^3}{T + (l) T^3}; \quad (7)$$

where we have expanded  $\kappa_{el}$  and  $\kappa_{ph}$  up to the lowest order in temperatures as  $\kappa_{el} \propto T$  and  $\kappa_{ph} \propto (l) T^3$ . The prefactor and  $(l)$  are  $\kappa_{el} = 2^2 k_B^2 \Gamma(E) = (3h)$  and  $(l) = 8^5 k_B^4 C^2 A^2 Y^2 = (15 \cdot l^2)$ , respectively. One may notice that there is a characteristic temperature  $T_0 = \frac{\kappa_{ph}}{\kappa_{el}} = (l)$ , which is around 10 K for the alkanethiol-molecular junctions and is negligibly small for aluminum-atomic junctions. When  $T \ll T_0$ , the electron thermal conductance dominates and  $ZT \propto S^2 T = \kappa_{el}^{-2} T^2$ , which is irrelevant to the length-characteristic of the junction and is proportional to  $T^2$  as temperatures increase. When  $T \gg T_0$ , the phonon thermal conductance dominates and  $ZT$  tends to have a saturation value of  $ZT \propto S^2 T = \kappa_{ph}^{-2} T^3 = (l)$ , which is related to the length of the junction. The above analytic expressions provide a convenient means for analyzing the length characteristic of  $S$  and  $ZT$  in nanojunctions.

Before turning to the detailed discussion on the thermoelectric properties in nanojunctions, we must draw attention to the reason why nanojunctions display material properties for  $S$  and  $ZT$ . The Seebeck coefficients are directly related to the transmission functions, which are determined by the electronic structures of the crystal materials irrelevant to the size and shape of the material, leading to the material properties for  $S$ . Furthermore, the conductance and the combined thermal conductance  $\kappa = \kappa_{el} + \kappa_{ph}$  are proportional to the contact surface and inversely proportional to the length scale in the bulk crystal materials, which leads to the material properties for  $ZT$  due to the cancelation of the geometric factors in the conductance and the combined thermal conductance. However, whether the thermoelectric materials in nanojunctions remain to display material properties or show junction properties have not yet been fully realized.

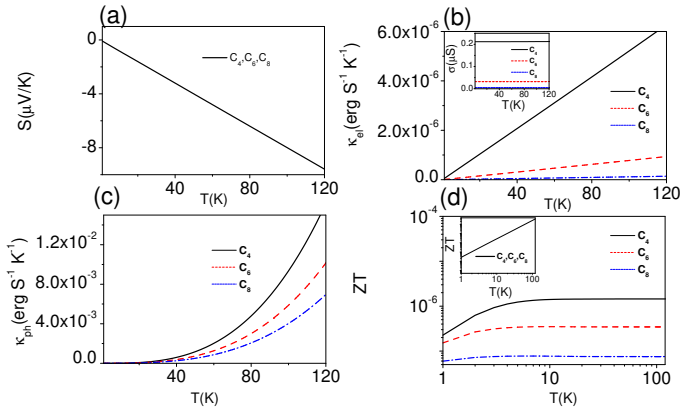


FIG. 1: (color online) Alkanethiol junctions at  $V_B = 0.01$  V for  $C_4$  [solid (black) lines],  $C_6$  [dotted-dash (red) lines], and  $C_8$  [dash (blue) lines]: (a) the Seebeck coefficient  $S$  vs.  $T$ ; (b) the electron thermal conductivity  $\kappa_{el}$  and the electrical conductivity (inset) vs.  $T$ ; (c) the phonon thermal conductivity  $\kappa_{ph}$  vs.  $T$ ; and (d) the log-log plot of  $ZT$  vs.  $T$  (inset shows the case of neglecting the thermal conductivity  $\kappa_{ph} = 0$ ).

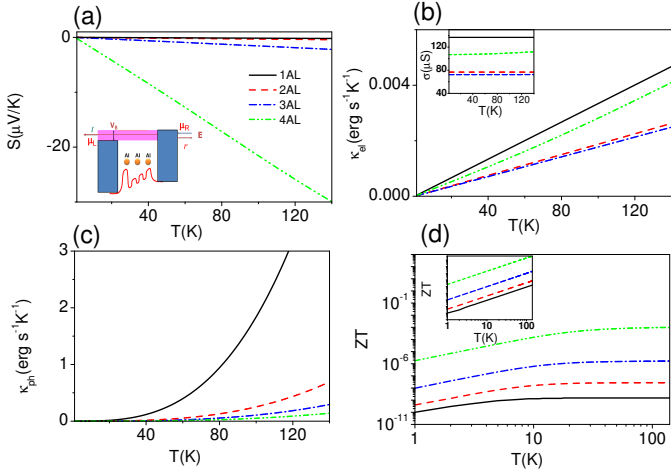


FIG. 2: (color online) Aluminum atomic junctions at  $V_B = 0.01$  V for 1 Al [solid (black) lines], 2 Al [dotted-dash (red) lines], 3 Al [dash (blue) lines], and 4 Al [dot-dot-dash (green) lines]: (a) the Seebeck coefficient  $S$  vs.  $T$  and the schematic of 3-Al atomic chain and its energy diagram (inset) where the Al-Al bond distance is about 6.3 a.u.; (b) the electron thermal conductivity  $\kappa_{el}$  and the electrical conductivity (inset) vs.  $T$ ; (c) the phonon thermal conductivity  $\kappa_{ph}$  vs.  $T$ ; (d) the log-log plot of  $ZT$  vs.  $T$  (inset shows the case of neglecting the thermal conductivity  $\kappa_{ph} = 0$ ).

Now, let us look closely into the properties of  $S$  and  $ZT$  in the linear response regime at low temperatures with  $T = T_L = T_R$  for the two catalogs of nanojunctions: the (insulating) alkanethiol junctions and the (metallic) aluminum atomic junctions.

First, we examine the dependence of  $S$  and  $ZT$  on the lengths of the alkanethiol junctions [17]. Alkanethiols [ $\text{CH}_3(\text{CH}_2)_{n-1}\text{SH}$ , denoted as  $C_n$ ] are a good example of reproducible junctions which can be fabricated [18, 19]. It has been well established that the non-resonant tunneling is the main conduction mechanism in the  $C_n$  junctions.

As shown in the inset of Fig. 2(b), the conductance is small, insensitive to temperatures, and decreases exponentially with the length of the molecules, as  $G = G_0 \exp(-\beta l)$ , where  $l$  is the length of  $C_n$  molecule and  $G_0 = 78 \text{ \AA}^{-1}$  [20, 21, 22, 23, 24]. By exploiting the periodicity in the  $(\text{CH}_2)_2$  group of the  $C_n$  chains, the wave functions of the  $C_n$  junctions are calculated by a simple scaling argument, leading to exponential scaling in the transmission functions (Eq. 1). It must be noted that the Seebeck coefficients are proportional to  $\frac{e \langle \epsilon \rangle = eE}{k_B T}$ . Consequently, the Seebeck coefficient does not show dependence on the length [see Fig. 1(a)] of the  $C_n$  junctions due to the cancellation of the exponential scaling behavior in (Eq. 1) for insulating molecules. We have noted that the cancellation may not be complete in the real experiments; thus, the Seebeck coefficients could possibly show weak length dependence due to other effects [11, 12]. In such case, the Seebeck coefficients mostly display material properties.

Let us now investigate the length-dependence of  $ZT$  for the  $C_n$  junctions. We predict that the  $C_n$  junctions display the material properties when  $T \ll T_0$  and display the junction properties when  $T \gg T_0$ . The reason for this is due to different scaling behaviors on the length characteristics of the junctions for the electron and phonon thermal conductivity and the competition between them. When  $T \ll T_0$ , the electron transport dominates the thermal current, and thus  $ZT \approx S^2 T = \kappa_{el}^{-1}$ . As shown in the inset of Fig. 1(d),  $ZT$  is independent from the lengths of  $C_n$  molecules and displays material properties. This result can be explained quite naturally by the cancellation of the exponential scaling in  $\kappa_{el}$  and  $\kappa_{ph}$  because both the electric current (with conductance  $G$ ) and the electron thermal current (with thermal conductivity  $\kappa_{el}$ ) are conveyed by electron transport. When  $T \gg T_0$ , the phonon transport dominates the thermal current and thus  $ZT \approx S^2 T = \kappa_{ph}^{-1}$ . As shown in the main body of Fig. 1(d),  $ZT \propto l^2 \exp(-\beta l)$  because of  $G \propto \exp(-\beta l)$  [see the inset of Fig. 1(b)], and  $\kappa_{ph} \propto l^2$  [see Fig. 1(c)]. In this case,  $ZT$  displays junction properties.

Finally, we will examine the dependence of  $S$  and  $ZT$  on the lengths of the metallic aluminum (Al) atomic junctions [17]. An Al atomic chain is an ideal testbed for studying the charge transport at the atom-scale level [see the inset of Fig. 2(a) for a schematic of the aluminum atomic junction] [25, 26, 27, 28]. This study has observed that  $S$  and  $ZT$  depend on the geometric characteristic of the junctions and show the junction properties in any case, which is in sharp contrast to the  $C_n$  junctions. At a fixed temperature, it has been observed that  $ZT$  and the magnitude of  $S$  increase as the number of Al atoms increases, as shown in Figs. 2(a) and (d). The increase of the Seebeck coefficients is due to the increase of the slopes in the transmission functions at the Fermi levels. The reason for this may be due to the strong hybridization between the electronic structures of atoms and the electrodes. The negative sign of the Seebeck coefficients indicates that the metallic Al atomic junctions are n-

type [the Fermi energy is closer to the lowest unoccupied molecular orbital (LUMO)].

In conclusion, this study has raised and answered an important fundamental question in thermoelectric nanojunctions: do the thermoelectric materials in nanojunctions remain to display material properties or show junction properties? To answer this question, we have developed a theory with analytical expressions for  $S$  and  $ZT$  allied to a fully self-consistent first-principles calculation in the DFT framework. Using the insulating alkanethiol molecular junctions and metallic aluminum junction as examples, this study concludes that the thermoelectric quantities in nanojunctions do not necessarily display material properties or junction properties. The metallic atomic chains reveal strong length characteristics related to the strong hybridization in the electronic structures between the atoms and electrodes, while the insulating molecular wires display strong material properties due to the cancelation of exponential scalings in the DOSs. For  $S$ , the metallic atomic chains reveal strong length characteristics related to the strong interactions between the electronic structure of atoms and the electrodes, while the insulating molecular wires show independence from the lengths of molecules, thus displaying strong material properties due to the cancelation of exponential scalings in the density of states. It may be worth pointing out the cancelation may not be complete in real experiments due to other effects; the important point is, the strong exponential scaling behavior with the lengths of the junctions should be canceled. For  $ZT$ , the atomic wires remain to show strong junction properties. However, the length characteristics of the insulating molecular wires depends on a characteristic temperature  $T_0 = \frac{p}{k_B} = \frac{1}{\beta}$  around 10 K. When  $T < T_0$ , where the electron transport dominates the thermal current, the molecular junctions remain to show material properties. When  $T > T_0$ , where the phonon transport dominates the thermal current, the molecular junctions display junction properties. The length characteristic of the  $C_n$  molecules is according to  $ZT \propto L^2 \exp(-L)$ . The different length-scaling behaviors between the thermal current conveyed by the electrons and the thermal current conveyed by the phonons offer the key to the understanding of characteristic temperature and the behavior of  $ZT$ . We believe that this study is a substantial step towards the understanding of the thermoelectric properties in nanojunctions, and we hope that this study will generate more experimental and theoretical explorations in the properties of thermoelectric nanojunctions.

We are grateful to Prof. N. J. Tao for helpful discussions. The authors thank MOE ATU, NCTS and NCHC for support under Grants NSC 97-2112-M-009-011-M-Y3, 097-2816-M-009-004 and 97-2120-M-009-005.

- <sup>1</sup> M. Paulsson and S. Datta, Phys. Rev. B 67, 241403 (R), (2003).
- <sup>2</sup> X. Zheng, W. Zheng, Y. Wei, Z. Zeng and J. Wang, J. Chem. Phys. 121, 8537 (2004).
- <sup>3</sup> B. Wang, Y. Xing, L. Wan, Y. Wei and J. Wang, Phys. Rev. B 71, 233406 (2005).
- <sup>4</sup> M. Galperin, A. Nitzan and M. A. Ratner, Molecular Physics, 106, 397 (2008).
- <sup>5</sup> F. Pauly, J. K. Viljas and J. C. Cuevas, Phys. Rev. B 78, 035315 (2008).
- <sup>6</sup> C. M. Finch, V. M. Garcia-Suarez and C. J. Lambert, Phys. Rev. B 79, 033405 (2009).
- <sup>7</sup> T. Markussen, A. P. Jauho and M. Brandbyge, Phys. Rev. B 79, 035415 (2009).
- <sup>8</sup> D. Yonatan and M. DiVentra, Nano Lett. 9, 97 (2009).
- <sup>9</sup> S. H. Ke, W. Yang, S. Curtarolo and H. U. Baranger, Nano Lett. 9, 1011 (2009).
- <sup>10</sup> Y. S. Liu and Y. C. Chen, Phys. Rev. B (2009) (in press).
- <sup>11</sup> P. Reddy, S. Y. Jang, R. A. Segalman and A. Majumdar, Science 315, 1568 (2007).
- <sup>12</sup> K. Baheti, J. A. Malen, P. D. Oak, P. Reddy, S. Y. Jang, T. D. Tilley, A. Majumdar and R. A. Segalman, Nano Lett. 8, 715 (2008).
- <sup>13</sup> J. A. Malen, P. D. Oak, K. Baheti, T. D. Tilley, R. A. Segalman and A. Majumdar, Nano Lett. 9, 1164 (2009).
- <sup>14</sup> N. D. Lang, Phys. Rev. B 52, 5335 (1995); M. DiVentra and N. D. Lang, Phys. Rev. B 65, 045402 (2001).
- <sup>15</sup> Y. C. Chen and M. DiVentra, Phys. Rev. Lett., 95, 166802 (2005).
- <sup>16</sup> K. R. Patton and M. R. Geller, Phys. Rev. B 64, 155320 (2001).
- <sup>17</sup> The aluminum (alkanethiol) junction consisted of an Al atomic chain (a  $C_4$  molecule) sandwich between two Al (Au) electrodes that were modeled as electron jellium with  $r_s = 2$  ( $\approx 3$ ). The following parameters were used for the junctions: the effective cross-section chosen was  $A = 23.1 \text{ a.u.}^2$  ( $21.4 \text{ a.u.}^2$ ) for the aluminum (alkanethiol) junction. The spectral densities of electrodes were evaluated using the longitudinal and transverse sound velocities for Al (Au),  $v_l = 6.35$  ( $3.2$ )  $10^6 \text{ cm/s}$  and  $v_t = 3.1$  ( $1.2$ )  $10^6 \text{ cm/s}$ , respectively. The Young's modulus of aluminum (alkanethiol) wire,  $Y = 1.2 \times 10^{11} \text{ dyne/cm}^2$  ( $Y = 2.3 \times 10^{11} \text{ dyne/cm}^2$ ), was calculated with total energy calculations and was found to be almost independent of the length of the wires.
- <sup>18</sup> W. Wang, T. Lee and M. A. Reed, Phys. Rev. B 68, 035416 (2003).
- <sup>19</sup> N. J. Tao, Nat. Nanotechnol., 1, 173 (2006).
- <sup>20</sup> D. J. Wold and C. D. Frisbie, J. Am. Chem. Soc., 123, 5549 (2001).
- <sup>21</sup> J. M. Beebe, V. B. Engelkes, L. L. Miller and C. D. Frisbie, J. Am. Chem. Soc., 124, 11268 (2002).
- <sup>22</sup> J. Zhao and K. Uosaki, Nano Lett., 2, 137 (2002).
- <sup>23</sup> C. C. Kuo and H. Guo, Nano Lett., 3, 1521 (2003).
- <sup>24</sup> C. L. Ma, D. N. Ghem and Y. C. Chen, Appl. Phys. Lett. 93, 222111 (2008).
- <sup>25</sup> N. D. Lang and Ph. A. P. Vouris, Phys. Rev. Lett. 81, 3515 (1998).
- <sup>26</sup> N. Kobayashi, M. Brandbyge and M. T. Sukada, Phys. Rev. B 62, 8430 (2000).
- <sup>27</sup> Z. Yang, M. Chshiev, M. Zwolak, Y. C. Chen and M. DiVentra, Phys. Rev. B 71, 041402 (R) (2005).
- <sup>28</sup> J. C. Cuevas, A. Levy Yeyati, A. Martin-Rodero, G. R. Bollinger, C. Untiedt and N. A. Graff, Phys. Rev. Lett. 81, 2990 (1998).